https://doi.org/10.5194/egusphere-2024-4010
Preprint. Discussion started: 25 February 2025


# Improving wheat phenology and yield forecasting with a deep learning-enhanced WOFOST model under extreme weather conditions

Jinhui Zheng[1], Le Yu[1,2,3,*], Zhenrong Du[4], and Liujun Xiao[5]

[1]Department of Earth System Science, Ministry of Education Key Laboratory for Earth System Modeling, Institute for Global Change Studies, Tsinghua University, Beijing 100084, China
[2]Ministry of Education Ecological Field Station for East Asian Migratory Birds, Beijing 100084, China
[3]Tsinghua University (Department of Earth System Science)- Xi'an Institute of Surveying and Mapping Joint Research Center for Next-Generation Smart Mapping, Beijing 100084, China
[4]School of Information and Communication Engineering, Dalian University of Technology, Dalian 116024, China
[5]College of Agriculture, Nanjing Agricultural University, Nanjing 210095, China

*Correspondence to*: Le Yu (leyu@tsinghua.edu.cn)

**Abstract.** Extreme weather events pose significant challenges to crop production, making their assessment essential for developing effective climate adaptation strategies. Process-based crop models are valuable for evaluating climate change impacts on crop yields but often struggle to simulate the effects of extreme weather accurately. To fill this knowledge gap, this study introduces WOFOST-EW model, an enhanced version of the World Food Studies Simulation Model (WOFOST), which integrates extreme weather indices and deep learning algorithm to improve simulations of winter wheat growth under extreme conditions. We validate WOFOST-EW using phenological, yield, and extreme weather data from agricultural meteorological stations in the North China Plain. The results show that WOFOST-EW improves simulation accuracy, with heading and maturity dates predicted more accurately by 10.64 % and 12.86 %, respectively. The $R^2$ value for yield simulations increases from 0.67 to 0.76. Validation during extreme weather years (2008 and 2018) further highlights the model's improved performance, with the $R^2$ increasing from 0.69 to 0.79 in 2008 and from 0.61 to 0.80 in 2018, respectively. WOFOST-EW effectively captures the impacts of extreme weather, offering a reliable tool for agricultural planning and climate adaptation. As extreme weather events become increasingly frequent, WOFOST-EW can assist decision-makers in more accurately evaluating crop yields, providing technical support for agricultural systems in the context of global climate change.

## 1 Introduction

Climate change is one of the most important determinants of crop yield, explaining 30-50 % of global yield variability (Ray et al., 2015; Rezaei et al., 2018). Extreme weather events driven by climate change are increasingly frequent and have become a major factor causing fluctuations in crop yields and declines in agricultural income (Lobell et al., 2011; Lesk et al., 2016;

https://doi.org/10.5194/egusphere-2024-4010
Preprint. Discussion started: 25 February 2025


Powell and Reinhard, 2016; Shen et al., 2022). In the future, the frequency and intensity of extreme weather events such as droughts, floods, and heatwaves are expected to rise, further stressing agricultural production (Bai et al., 2022).

China is a major producer of wheat globally, with a wheat production of 137 million tons in 2021, accounting for 17.8 % of the world's total production (FAO, 2021). Wheat plays a crucial role globally in food security, economy, agriculture, and culture (Beyene et al., 2022; Erenstein et al., 2022; Reynolds et al., 2022). The North China Plain is the primary wheat-producing region in China, contributing to more than 50 % of the national output (Xiao et al., 2020). This region is highly vulnerable to climate change impacts (Hu et al., 2014), with the frequency of climate anomalies increasing since 1980 (Mo et al., 2017). Extreme weather events significantly affect wheat production in the North China Plain. Winter wheat, typically sown in October or November and harvested in May or June, is particularly vulnerable to drought during its growing season (Chen et al., 2018; Li et al., 2021). During winter, wheat grows slowly or remains dormant, making it less sensitive to climate change. However, in spring, it grows rapidly and becomes more sensitive to extreme weather such as drought or low temperatures (Shi et al., 2011; Ali et al., 2017). Moreover, wheat is highly susceptible to frost during the jointing and booting stages (Li et al., 2014), with each additional day of frost causing a 4.3-6.7 % reduction in grain yield (Ji et al., 2017). Excessive rainfall and insufficient sunlight in May and June, often linked to flooding, diseases, and pests, further reduce both the yield and quality of wheat (Song et al., 2019). As a result, accurately estimating crop yields under extreme weather conditions is crucial for assessing agricultural sustainability.

Currently, scholars worldwide have proposed various methods to estimate crop yields. Many studies use statistical regression models to investigate the relationship between climate change and crop yields (Tao et al., 2012; Zhang et al., 2017a; Ai et al., 2020; Li et al., 2020; Lu and Yang, 2021; Ringeval et al., 2021; Dinh and Aires, 2022; Wang et al., 2022; Ai and Hanasaki, 2023; Wei et al., 2023). The main advantage of statistical models is their relatively low dependence on field calibration data, and their ability to transparently assess model uncertainty through higher coefficients of determination and narrower confidence intervals (Lobell and Burke, 2010). Current research primarily focuses on combining climate variables with yield data to develop linear regression models, in order to quantify the role of climate variables in yield variations (Tao et al., 2012; Zhang et al., 2017a; Li et al., 2020; Wang et al., 2022; Wei et al., 2023). However, only a few studies have considered the multicollinearity characteristics of climate variables (Li et al., 2020; Wang et al., 2022). Given the complexity of climate change impacts on crop growth, it is necessary to consider their nonlinear characteristics. Compared to linear regression models, machine learning algorithms significantly improve the accuracy of crop yield simulations (Khanal et al., 2018). Machine learning algorithms are advanced methods for exploring the relationships between climate and yield, capable of capturing hierarchical and nonlinear relationships between predictors and response variables. Numerous studies have demonstrated the effectiveness of machine learning in crop yield estimation (Wang et al., 2018; Maimaitijiang et al., 2019; Han et al., 2020; Sun

https://doi.org/10.5194/egusphere-2024-4010
Preprint. Discussion started: 25 February 2025


et al., 2020; Wang et al., 2020; Cao et al., 2021; Tian et al., 2021; Boori et al., 2022; Ruan et al., 2022; Iniyan et al., 2023; Singh Boori et al., 2023; Torsoni et al., 2023). However, both statistical models such as linear regression and machine learning models focus on establishing correlations between climate and yield data, neglecting the physiological and ecological processes of crops and failing to fully consider the mechanisms of crop growth (Roberts et al., 2017; Zhao et al., 2022; Bai et al., 2024; Xiao et al., 2024).

Process-based crop models have been developed to explain the complex interactions between local environments, crop genotypes, and management practices (Chenu et al., 2017). Compared to statistical models, process-based crop models are mechanistic, flexible, and applicable (Zhang et al., 2017b; Tang et al., 2023; Zheng and Zhang, 2023; Jing et al., 2024). However, most crop models are developed under relatively stable climatic conditions. The impacts of extreme climate on crop yields are overly simplified and vaguely described in crop models, resulting in inaccurate simulation results under extreme climatic conditions (Feng et al., 2019; Bai et al., 2024; Yu et al., 2025; Zheng and Zhang, 2025). This also leads to global process-based crop models often underestimating the magnitude of crop yield losses caused by extreme heatwaves and excessive rainfall (Liu et al., 2020; Heinicke et al., 2022; Fu et al., 2023).

Given the limitations of crop models and statistical regression models, some studies have combined crop models with machine learning to achieve better yield prediction results. Li et al. (2023) improved the accuracy and reduced uncertainty in predicting corn and soybean yields under extreme weather by combining machine learning algorithms with nine global gridded crop models. Feng et al. (2019) incorporated APSIM model outputs and extreme climate indicators into a random forest algorithm, resulting in improved model prediction accuracy. Shahhosseini et al. (2021) coupled crop model outputs with machine learning models to enhance crop yield predictions in the U.S. corn belt. However, most previous studies simply input crop model outputs into machine learning models, overlooking some key dynamic changes in crop growth processes, especially under extreme weather events. Furthermore, these methods lack accuracy and robustness in dealing with the impact of extreme weather on crop yields, failing to fully capture the effects of extreme weather on crop growth.

In this study, we introduce WOFOST-EW, an enhanced version of the WOFOST (World Food Studies Simulation Model) model that integrates extreme weather indices and the Long Short-Term Memory (LSTM) algorithm to improve simulations of winter wheat growth under extreme conditions. The main objectives of the research are (1) Calibration and validation of the WOFOST model using wheat yield and phenology data from the North China Plain for the period 1980-2020; (2) Evaluate the simulation performance of WOFOST-EW in yield and phenology; (3) Validation in agricultural meteorological station impacted by extreme weather to assess the model's robustness.

https://doi.org/10.5194/egusphere-2024-4010
Preprint. Discussion started: 25 February 2025


## 2. Materials and methods

### 2.1 Study areas

The North China Plain (Fig. 1) features a warm temperate continental monsoon climate, characterized by abundant sunlight and warmth, although precipitation is unevenly distributed, with the majority falling during the summer months (June to August). The predominant soil type in the North China Plain is aeolian soil deposited over geological periods by rivers. This study focuses on wheat cultivation in the North China Plain, the second-largest plain in China, which plays a crucial role in grain production. The dominant cropping system in this region is a double-cropping system of winter wheat and summer maize. Winter wheat is typically sown in early October and harvested in June, requiring substant uts of water and fertilizers. To ensure data quality and integrity, we selected 25 counties for this research (Fig. 1). Table 1 provides detailed information on the crops and climate at these research stations.

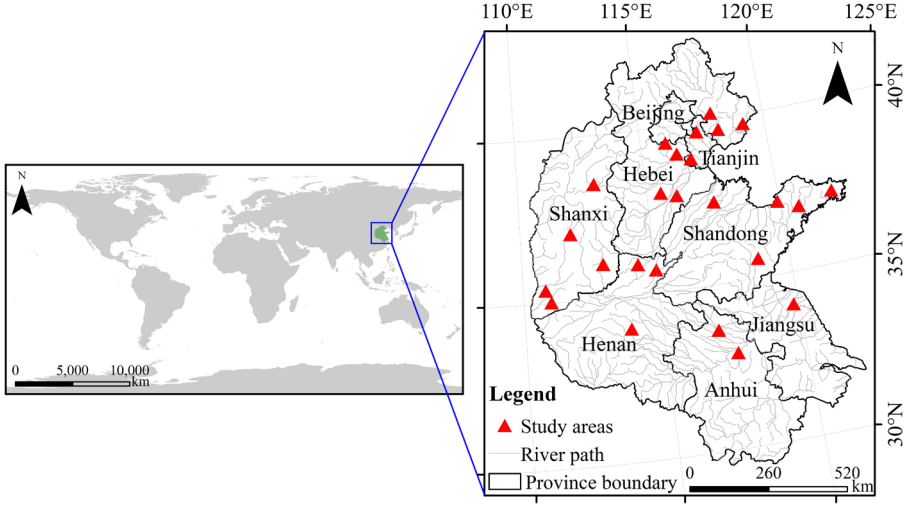


**Figure 1.** Location of the study areas.

**Table 1.** Details of the agricultural meteorological experiment stations.

| Counties | Longitude | Latitude | Climate type | Annual precipitation (mm) | Annual mean temperature (°C) |
|---|---|---|---|---|---|
| Tangshan | 118.2 °E | 39.7 °N | Temperate continental | 976.0 | 12.2 |

https://doi.org/10.5194/egusphere-2024-4010
Preprint. Discussion started: 25 February 2025


| | | | | | |
|---|---|---|---|---|---|
| Jinghai | 116.9 °E | 38.9 °N | Warm temperate continental | 484.4 | 13.3 |
| Zunhua | 118.0 °E | 40.2 °N | Temperate continental | 800.0 | 11.9 |
| Shenzhou | 115.6 °E | 38.0 °N | Warm temperate semi-arid | 486.0 | 12.8 |
| Zhuozhou | 116.0 °E | 39.5 °N | Warm temperate continental | 554.1 | 12.7 |
| Baodi | 117.3 °E | 39.7 °N | Warm temperate semi-humid | 612.5 | 13.3 |
| Xuchang | 113.9°E | 34.0°N | Warm temperate monsoon | 683.9 | 14.7 |
| Yuncheng | 111.0 °E | 35.0 °N | Temperate monsoon | 525.0 | 14.6 |
| Binhai | 119.8 °E | 34.0 °N | Warm temperate semi-humid | 964.8 | 14.5 |
| Tangyin | 114.4 °E | 35.9 °N | North temperate continental | 588.9 | 14.3 |
| Laizhou | 119.9 °E | 37.2 °N | Warm temperate continental | 810.7 | 13.7 |
| Changli | 119.2 °E | 39.7 °N | Warm temperate semi-humid | 527.0 | 11.4 |
| Puyang | 115.0 °E | 35.7 °N | Subtropical monsoon | 643.1 | 13.6 |
| Jiexiu | 111.9 °E | 37.1 °N | Temperate monsoon | 477.2 | 12.6 |
| Fengyang | 117.6 °E | 32.9 °N | Subtropical monsoon | 904.4 | 16.7 |
| Wendeng | 122.0 °E | 37.2 °N | Temperate maritime | 803.9 | 12.9 |
| Dingxiang | 113.0 °E | 38.5 °N | Warm temperate semi-humid | 471.9 | 9.8 |
| Huimin | 117.5 °E | 37.5 °N | Temperate monsoon | 582.3 | 13.1 |
| Bazhou | 116.4 °E | 39.1 °N | Temperate continental | 479.4 | 12.7 |
| Wanrong | 110.8 °E | 35.4 °N | Temperate continental | 983.6 | 14.6 |
| Changzhi | 113.1 °E | 36.1 °N | Warm temperate semi-humid | 512.5 | 10.1 |
| Laiyang | 120.7 °E | 36.9 °N | Temperate monsoon | 764.0 | 13.2 |
| Fucheng | 116.2 °E | 37.9 °N | Temperate monsoon | 588.0 | 13.6 |
| Suzhou | 117.0 °E | 33.6 °N | North temperate monsoon | 840.0 | 14.5 |
| Juxian | 118.8 °E | 35.6 °N | Warm temperate monsoon | 750.5 | 12.1 |

## 2.2 Datasets

### 2.2.1 WOFOST input data

The input data for the WOFOST model includes weather, crop, soil, and management parameters. The meteorological data used in this study was sourced from the United States National Centers for Environmental Information

https://doi.org/10.5194/egusphere-2024-4010
Preprint. Discussion started: 25 February 2025


(https://www.ncei.noaa.gov), providing key climate data from 1980 to 2020. This data covers meteorological observation stations across the country and undergoes strict quality control and validation, ensuring high reliability and usability. Agricultural management data was obtained from agricultural meteorological stations of the China Meteorological Administration (https://www.cma.gov.cn), and soil data were obtained from the ISRIC global database (https://www.isric.org), encompassing soil type, profile depth (cm), bulk density (cg/cm3), cation exchange capacity (mmol/kg), volumetric fraction of coarse fragments (cm3/dm3), clay content (g/kg), total nitrogen content (cg/kg), etc. The depth of the soil profile was categorized into intervals: 0-5 cm, 5-15 cm, 15-30 cm, 30-60 cm 60-100cm, and 100-200 cm.

#### 2.2.2 Yield data

The county-level wheat yields time series data from 1980 to 2020 were sourced from the Agricultural Yearbook of each province (https://www.stats.gov.cn, autonomous region, municipality directly under the Central Government), supplemented by data not publicly disclosed by county-level survey bureaus and data from agricultural meteorological stations of the China Meteorological Administration.

#### 2.2.3 Extreme weather data

The extreme weather data used in this study was sourced from the Yearbook of Meteorological Disasters in China (https://data.cma.cn) and previous research (Yin et al., 2017; Wang et al., 2019; Zhao et al., 2019; Wang et al., 2021; Bai et al., 2022; Yang et al., 2022; Guo et al., 2024). It comprehensively records the occurrence of various extreme weather in China, including typhoons, heavy rainfall, droughts, strong winds, snow disasters, etc. The yearbook provides statistics on the frequency of extreme weather, affected areas, population impact, and the resulting economic losses. Table S1 contains information in the counties affected by extreme weather.

### 2.3 Methods

#### 2.3.1 SCE-UA algorithm

This study utilized the Shuffled Complex Evolution Algorithm (SCE-UA) developed by the University of Arizona to find the optimal parameter combinations for the WOFOST model. The algorithm was implemented for model calibration using the "spotpy" package in Python. The SCE-UA algorithm iterates the WOFOST model to minimize the cost function. Proposed by Duan et al. (Duan et al., 1992; Duan et al., 1993), the algorithm combines the advantages of deterministic search, random search, and competitive evolution algorithms, and has been proven to perform excellently in global search and multi-parameter combination optimization. A notable feature of SCE-UA is its insensitivity to initial values, enhancing the model's applicability in different scenarios (Duan et al., 1994; Huang et al., 2018).

https://doi.org/10.5194/egusphere-2024-4010
Preprint. Discussion started: 25 February 2025


### 2.3.2 Climate indices

We quantified the impact of extreme weather on wheat production using seven metrics (Table 2). Among these, the HDD and LDD are widely used in studies on crops such as rice and wheat, as they reflect the influence of extreme weather on crop growth (Zhang et al., 2016; Zhang and Tao, 2019; Osman et al., 2020; Dong et al., 2023). The methods for calculating HDD and LDD follow those outlined in previous research (Osman et al., 2020).

Previous studies have shown that wheat exhibits varying sensitivity to temperature during different developmental stages (Porter and Gawith, 1999; Tack et al., 2015). Based on prior research (Porter and Gawith, 1999; Farooq et al., 2011; Liu et al., 2013), we set the high-temperature thresholds for wheat at 25 °C from planting to heading and 30 °C from heading to maturity. The low-temperature thresholds were defined as -5.7 °C for planting to heading and -2 °C for heading to maturity.

The calculations for R95P, R10mm, and Rx1day were based on the ETCCDI indices, as applied in previous studies (Hong and Ying, 2018; Al-Sakkaf et al., 2024). Data for the PDSI and VPD (Zhang and Miao, 2024) were spatially processed to extract site-specific values.

### 2.3.3 Deep learning algorithm

LSTM algorithm is a type of recurrent neural network (RNN) known for its stable and high-performance capabilities in long-term prediction tasks. It was first proposed by Sepp and Jürgen in 1997 to address the error back-flow problems (Kalchbrenner et al., 2019). This study utilizes the "Keras" library in Python to implement LSTM, which is distinguished by its multiple self-parameterizing control gates. These gates facilitate the selective storage and exclusion of information, allowing for the accumulation of specific data units.

**Table 2.** Definition of extreme weather indices.

| Extreme indices | Index | Definition | Unit |
|---|---|---|---|
| High-temperature degree days | HDD | Cumulative temperature exceeding the threshold during a specific growth period. | °C d |
| Low-temperature degree days | LDD | Cumulative temperature below the threshold during a specific growth period. | °C d |
| Very wet days | R95P | Annual total precipitation from days >95th percentile | mm |
| Heavy precipitation days | R10mm | Annual count when precipitation is 10 mm | d |

https://doi.org/10.5194/egusphere-2024-4010
Preprint. Discussion started: 25 February 2025


| | | | |
|---|---|---|---|
| Max 1-day precipitation amount | Rx1day | Annual maximum 1-day precipitation | mm |
| Palmer Drought Severity Index | PDSI | A standardized index to assess long-term soil moisture and drought conditions. | - |
| Vapor pressure deficit | VPD | The difference between the saturation vapor pressure and actual vapor pressure, indicates dryness. | kPa |

We developed a 5-layer deep neural network model comprising an input layer, two LSTM layers, a dense layer, and an output layer (Fig. 2). The input data include seven extreme weather indices values for the winter wheat growth period. The model's output predicts the value of the extreme weather function. To prevent overfitting, a dropout mechanism is applied to the input of the dense layer. The number of hidden nodes is determined on a case-by-case basis as there is no general rule for this. We used the "GridSearchCV" method (Kalchbrenner et al., 2019; Panigrahy, 2024) to determine optimal values for dropout and hidden nodes. For network parameter optimization, we employed the Adam optimizer based on gradient descent, using a learning rate of 0.001. We applied leave-one-year-out cross-validation, where data from one year are excluded from the test set, and the remaining years are used for training. This method evaluates the model's robustness under different climate and environmental conditions, ensuring reliable performance over time (Ma et al., 2021; Ji et al., 2022; Pei et al., 2025).

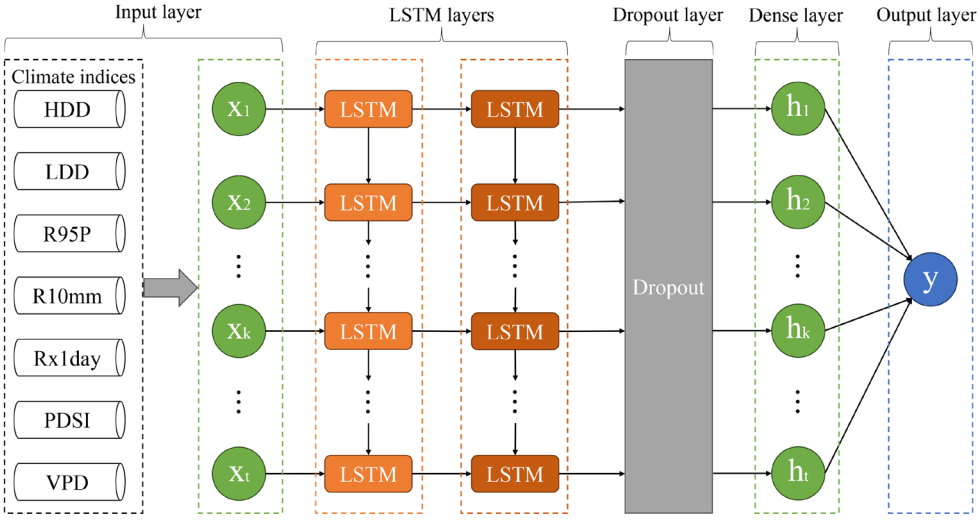


**Figure 2.** The workflow of a Long Short-Term Memory (LSTM) network.

https://doi.org/10.5194/egusphere-2024-4010
Preprint. Discussion started: 25 February 2025


### 2.3.4 WOFOST model improvement protocol

The WOFOST model, developed by Wageningen University in the Netherlands in collaboration with the World Food Studies Center, is used to calculate the daily biomass accumulation of crops based on photosynthesis and its distribution across various crop components (De Wit et al., 2020). The model includes several modules, such as phenological development, $CO_2$ assimilation, respiration, dry matter allocation, leaf area development (source and sink limitations), soil water and nutrient balance, and more. The outputs of the WOFOST model include simulated total crop biomass, crop yield, leaf area, and crop water use efficiency. For a detailed description of the WOFOST calculation process, refer to the relevant literature (Supit et al., 1994; de Wit et al., 2018; De Wit and Boogaard, 2021).

Here, we utilized the Python Crop Simulation Environment (PCSE 6.0.6) framework to run the WOFOST crop growth model (Wofost72_WLP_CWB). The research flowchart is shown in Fig. 3. In the WOFOST, phenological development is guided by the daily thermal time (DTT). The Development Index (DVI) is characterized by a value of 0 at emergence, 1 at flowering, and 2 at maturity (De Wit et al., 2020). It is noteworthy that in WOFOST, crop emergence occurs when the cumulative daily effective temperature exceeds a specific threshold temperature for the crop. The calculation of *DVI* is accumulated from the Development Rate (*DVR*):

$$DVI_t = \sum_{i=0}^{i=t} DVR_i \tag{1}$$

where $DVI_t$ is the developmental index at day t, and $DVR_i$ is the developmental rate on the ith day from planting.

The calculation for *DVR* is:

$$\mathrm{DVR} = \frac{F(T)}{\sum T_i} \times F(V) \times F(P) \tag{2}$$

where *F(T)* represents the daily effective temperature, and $\sum T_i$ denotes the temperature sum required to complete stage i. *F(T)* is calculated as:

$$\mathrm{T} < T_b : F(T) = 0 \tag{3}$$

https://doi.org/10.5194/egusphere-2024-4010
Preprint. Discussion started: 25 February 2025


$$T_b < T < T_m: F(T) = T - T_b \quad (4)$$

$$T > T_m: F(T) = T_m \quad (5)$$

where $T_b$ refers to the base temperature below which phenological development stops, $T_m$ represents the maximum temperature beyond which phenological activity does not increase, and $T$ represents the average daily temperature.

The vernalization ($F(V)$) and photoperiod functions ($F(P)$) also affected the daily development of wheat. Each function is defined as follows:

$$F(V) = \frac{V - V_{base}}{V_{sat} - V_{base}}, (0 < F(V) < 1) \quad (6)$$

$$F(P) = \frac{P - P_c}{P_o - P_c}, (0 < F(P) < 1) \quad (7)$$

where $V_{base}$ represents the minimum vernalization requirement (lower threshold) for development, while $V_{sat}$ defines the maximum vernalization limit (upper threshold). $P_c$ represents the threshold for day length in development; when the day length falls below $P_c$, $F(P)$ equals 0. $P_o$ is the optimum day length for development, above which $F(P)$ equals 1.

In this study, we proposed an improved WOFOST model incorporating an extreme weather function, referred to as WOFOST-EW. We developed an extreme weather function ($F(EW)$) to enhance the DVI calculation of the WOFOST model. The calculation is as follows:

$$F(EW) = f_{LSTM}(HDD, LDD, R95P, R10mm, Rx1day, PDSI, VPD) \quad (8)$$

where $f_{LSTM}$ represents the LSTM algorithm, while HDD, LDD, R95P, R10mm, Rx1day, PDSI, and VPD respectively represent climate indices.

Finally, we applied $F(EW)$ to the WOFOST model and obtained the updated $DVR_{EW}$:

https://doi.org/10.5194/egusphere-2024-4010
Preprint. Discussion started: 25 February 2025


$$DVR_{EW} = \frac{F(T)}{\sum T_i} \times F(V) \times F(P) \times F(EW) \quad (9)$$

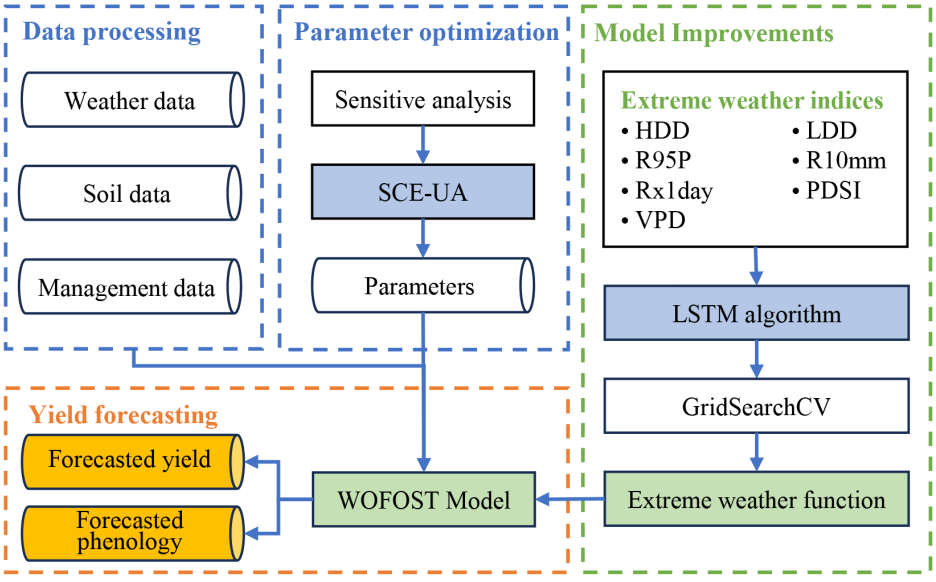


**Figure 3.** The program flowchart used in this study. HDD, LDD, R95P, R10mm, Rx1day, PDSI, and VPD represent different climate indices, and LSTM represents the Long Short-Term Memory algorithm.

### 2.3.5 Model calibration and validation

To enhance the performance of the crop model, calibration is essential. We utilized the SCE-UA algorithm to determine the optimal parameters [illegible]ch agricultural meteorol[illegible]station. These parameters are considered optimal when the Root Mean Square Error (RMSE) is minimized. The WOFOST parameters were calibrated using yield data from 1990 to 2000, and the optimal parameter sets were then applied to each simulated growing season at each location. The model was validated with data from 2001 to 2020. The simulation error was assessed by calculating the difference between observed and simulated yields. The detailed WOFOST parameters are provided in Table S2 of the Supplementary materials.

### 2.3.6 Model performance assessment

The performance of the model is evaluated by calculating the regression coefficients of determination ($R^2$), Pearson's rank correlation coefficient (Pearson's r), and RMSE using the following equations:

https://doi.org/10.5194/egusphere-2024-4010
Preprint. Discussion started: 25 February 2025


$$R^2 = 1 - \frac{\sum_{i=1}^{n}(y_i - \hat{y}_i)^2}{\sum_{i=1}^{n}(y_i - \bar{y})^2} \quad (10)$$

$$\text{Pearson's r} = \frac{\sum_{i=1}^{n}(y_i - \bar{y})(\hat{y}_i - \bar{\hat{y}})}{\sqrt{\sum_{i=1}^{n}(y_i - \bar{y})^2 \sum_{i=1}^{n}(\hat{y}_i - \bar{\hat{y}})^2}} \quad (11)$$

$$\text{RMSE} = \sqrt{\frac{\sum_{i=1}^{n}(y_i - \hat{y}_i)^2}{n}} \quad (12)$$

where $y_i$ is the observed value, $\hat{y}_i$ is the simulated value, and $n$ is the number of observations.

# 3 Results

## 3.1 Phenological simulation results

The phenological period simulation results for the 25 sites in the study area showed good performance in both the calibration and validation datasets (Fig. 4; Tables S3 and S4). In the calibration dataset (Fig. 4; Table S3), the WOFOST model's RMSE for heading ranged from 1.4 to 12.8 days, with an average of 5.7 days. The best-performing site was Jiexiu, while the worst-performing site was Fengyang. For the maturity period, the RMSE ranged from 3.1 to 13.1 days, with an average of 8.0 days. In comparison, The WOFOST-EW model's average RMSE results for heading and maturity periods were 4.2 days and 5.4 days, respectively.

In the phenological simulation results for the validation dataset (Fig. 4; Table S4), the RMSE for heading and maturity periods using the WOFOST model ranged from 1.0 to 9.5 days (average of 4.7 days) and from 3.2 to 11.8 days (average of 7.0 days), respectively. For the WOFOST-EW model, the RMSE for heading date simulations ranged from 1.0 to 6.0 days, with an average of 4.2 days, while for maturity date simulations, the RMSE ranged from 3.2 to 8.0 days, with an average of 6.1 days. The best and worst-performing sites for heading and maturity dates simulations using the WOFOST-EW model were Bazhou and Shenzhou, and Laiyang and Shenzhou, respectively.

Fig. 4c and d present box plots of the RMSE for heading and maturity dates simulated by the WOFOST and WOFOST-EW models. In the validation dataset, for the heading date, the lower and upper quartiles for the WOFOST model were 3.8 days and 5.5 days, respectively, while for the WOFOST-EW model, they were 3.9 days and 4.7 days (Fig. 4c). For the maturity date, the lower and upper quartiles for the WOFOST model were 5.4 days and 7.7 days (Fig. 4d), while for the WOFOST-EW model, they were 4.6 days and 7.0 days. These results indicate that, compared to the WOFOST model, the proposed WOFOST-

https://doi.org/10.5194/egusphere-2024-4010
Preprint. Discussion started: 25 February 2025


EW model significantly reduced the RMSE for both heading and maturity dates, thus improving accuracy. Furthermore, the smaller interquartile range suggests a narrower error range, indicating more stable and precise simulation results.

The WOFOST-EW model demonstrates improvements in both the accuracy and error range of phenological simulations compared to the WOFOST model, with prediction accuracy improving by 10.64 % during the heading stage and 12.86 % during the maturity stage in the validation dataset (Fig. 4).

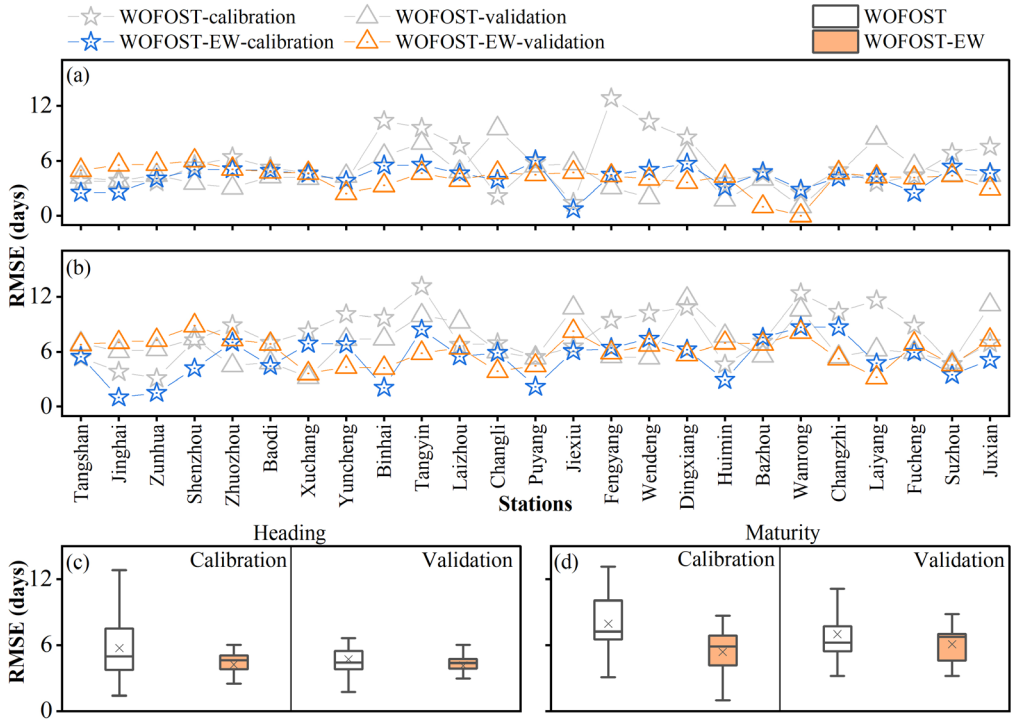


**Figure 4.** Simulation results of phenological stages for winter wheat using the WOFOST model and the WOFOST-EW model at 25 agrometeorological stations in the study area. (a) shows the Root Mean Square Error (RMSE) of simulated heading dates for the calibration and validation datasets at different stations for both models. (b) shows the RMSE of simulated maturity dates for the calibration and validation datasets at different stations for both models. (c) and (d) present boxplots of the RMSE for simulated heading and maturity dates, respectively. The × symbol represents the mean RMSE value, and the horizontal line within the box indicates the median (Q2). The box represents the interquartile range (IQR), with the top and bottom edges of the box denoting the upper quartile (Q3) and lower quartile (Q1), respectively. The whiskers extend to the maximum and minimum values, where the maximum value is defined as Q3 + 1.5 × IQR, and the minimum value is defined as Q1 – 1.5 × IQR.

https://doi.org/10.5194/egusphere-2024-4010
Preprint. Discussion started: 25 February 2025


### 3.2 Simulation results of yield

Despite some differences in simulation results across counties, the WOFOST model's simulated yields aligned well with observed yields (Figs. 5, 6, and 7; Tables S3 and S4). In the calibration dataset, the average RMSE in the simulated counties was 673.01 kg/ha (Figs. 5, and 6; Table S3). Among these, Dingxiang performed the best, with an RMSE of 555.83 kg/ha, while Changli showed poorer results, with an RMSE of 844.58 kg/ha. For the validation dataset, the RMSE of simulated yields by the WOFOST model ranged from 256.61 to 938.19 kg/ha, with an average RMSE of 665.76 kg/ha (Figs. 5, and 6; Table S4).

The improved WOFOST-EW model more accurately simulated winter wheat yields from 1980 to 2020 (Figs. 5, 6, and 7; Tables S3 and S4). In the calibration dataset, the RMSE for yield simulations ranged from 295.63 to 758.14 kg/ha, with an average of 541.90 kg/ha (Figs. 5 and 6; Table S3). In the validation dataset, the RMSE ranged from 279.64 to 960.75 kg/ha, with an average of 565.63 kg/ha (Figs. 5 and 6; Table S4).

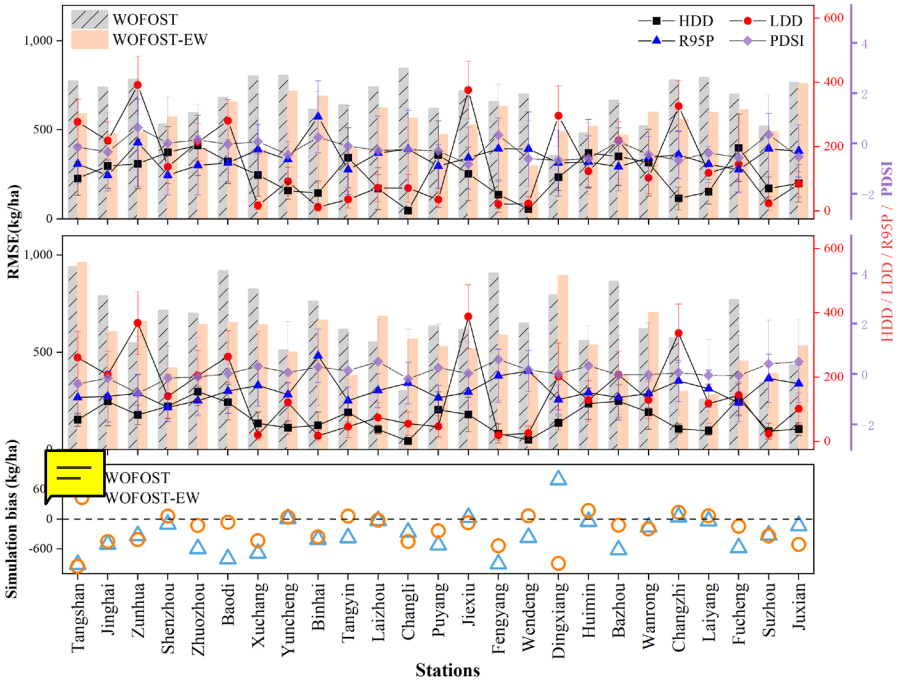


**Figure 5.** Root Mean Square Error (RMSE) values for winter wheat yield simulated by the WOFOST model and the WOFOST-EW model in the study area for the calibration dataset (a) and validation dataset (b). (c) illustrates the distribution of simulation errors for the two models.

https://doi.org/10.5194/egusphere-2024-4010
Preprint. Discussion started: 25 February 2025


HDD, LDD, and R95P represent climatic indices related to extremely high temperatures, low temperatures, and precipitation, respectively. PDSI represents the Palmer Drought Severity Index.

From 1990 to 2020, a comprehensive evaluation of annual yield simulations by the WOFOST model was performed (Fig. 6). The WOFOST model utilized a set of optimal parameters obtained through the SCE-UA method, allowing for effective simulation of wheat yields. In the WOFOST model, the mean absolute deviation (MAD) of the simulation results was 177.36 kg/ha, while the WOFOST-EW model reduced the MAD to 141.76 kg/ha (Fig. 6). Despite the overall high accuracy, errors were identified in yield simulations for certain years (Fig. 6b).

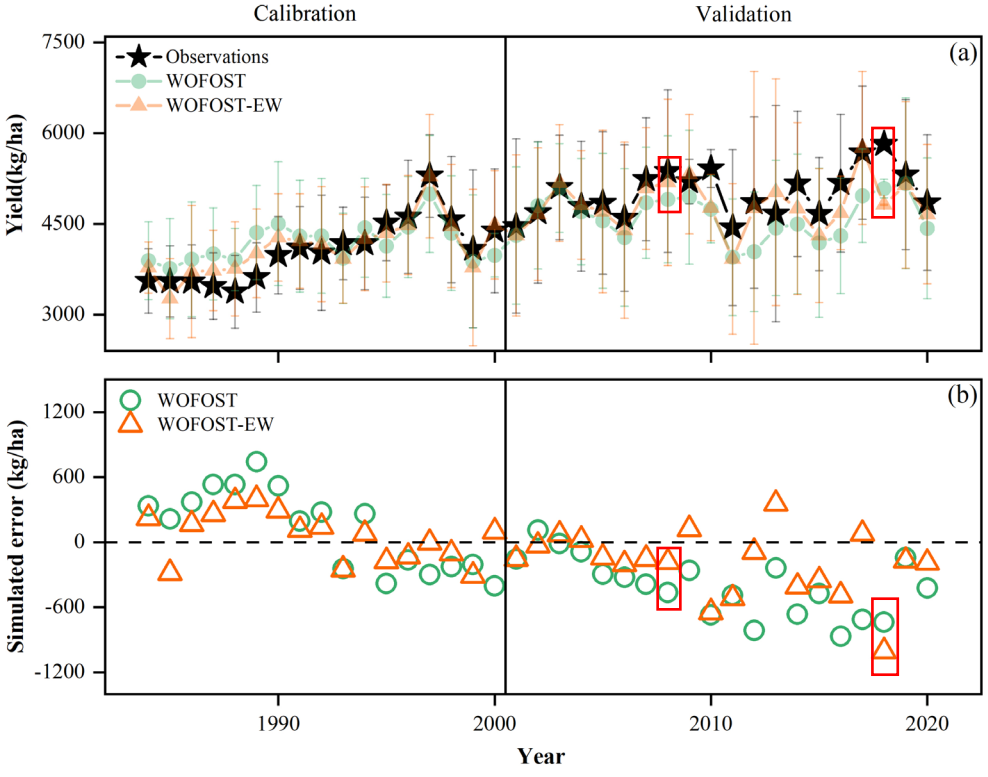


**Figure 6.** (a) Represent the winter wheat prediction results during the calibration and validation periods using the WOFOST and WOFOST-EW models. (b) Indicates the simulation errors of yield.

To further evaluate the performance of the two models, we analyzed the results for the validation dataset from 2001 to 2020 (Fig. 7). The simulation results of the WOFOST model showed a Pearson's r of 0.83, an RMSE of 665.76 kg/ha, and an $R^2$ of

https://doi.org/10.5194/egusphere-2024-4010
Preprint. Discussion started: 25 February 2025


0.67. In comparison, the WOFOST-EW model demonstrated enhanced yield estimation accuracy, with a Pearson's r of 0.86, a reduced RMSE of 565.63 kg/ha, and an improved $R^2$ of 0.76.

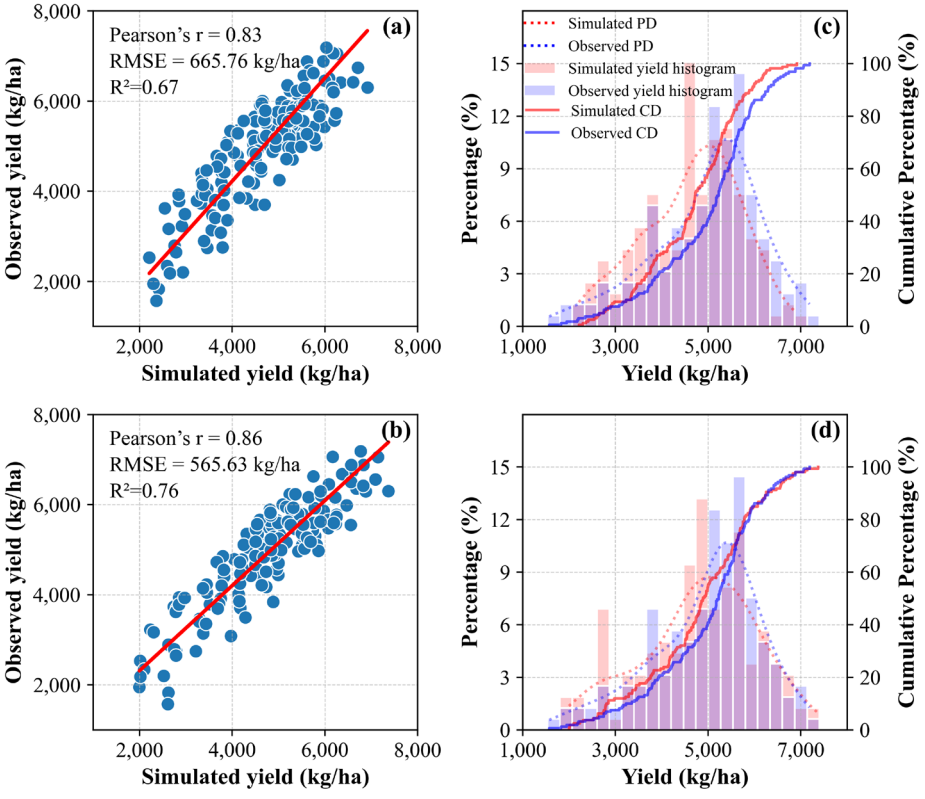


**Figure 7.** Comparison of simulated winter wheat yield distributions with observed yield records in the study area from 2000 to 2020. Subplots (a) and (c) show the comparison between the WOFOST model simulation results and observed yields; (b) and (d) display the comparison between the WOFOST-EW model results and observed yields. Here, PD denotes Probability Density, and CD denotes Cumulative Distribution.

### 3.3 Simulation analysis of counties affected by extreme weather

To further validate the effectiveness of the improved model, specific counties affected by extreme weather were selected for yield simulation. Table S1 provides detailed information about the counties impacted by extreme weather events in 2008 and 2018. The types of extreme weather observed in these counties included heavy rainfall and flooding, high-temperature drought, and frost (Table S1).

https://doi.org/10.5194/egusphere-2024-4010
Preprint. Discussion started: 25 February 2025


In 2008, ...me weather in the study area was primarily characterized by high temperatures and drought, particularly in some counties in Shanxi and Hebei (Table S1). The WOFOST model's simulation results yielded a Pearson's r of 0.83, an $R^2$ of 0.69, an RMSE of 799.99 kg/ha (Fig. 8a), and a MAD of 403.18 kg/ha (Fig. 9a). In comparison, the WOFOST-EW model demonstrated superior performance, achieving a Pearson's r of 0.91, an $R^2$ of 0.79, an RMSE of 617.05 kg/ha (Fig. 8b), and a MAD of 325.38 kg/ha (Fig. 9a).

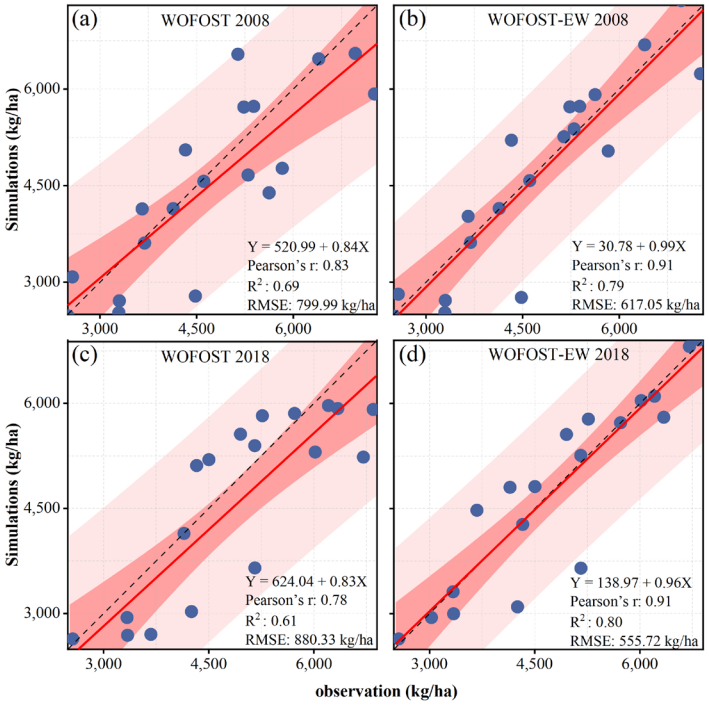


**Figure 8.** Comparison of simulated and observed records in the counties affected by extreme weath...008 and 2018. (a) and (b) illustrate the comparison between the WOFOST model, WOFOST-EW model simulations, and observed records for 2008. (c) and (d) depict the comparison between the WOFOST model, WOFOST-EW model simulations, and observed records for 2018.

In 2018, the primary extreme weather in the study area included heavy rainfall and increased low-temperature frost damage, indicating that climate change in recent years has led to more frequent extreme weather events, which have impacted agricultural production in various ways (Table S1). The WOFOST model's simulation results showed a Pearson's r of 0.78, an $R^2$ of 0.61, an RMSE of 880.33 kg/ha, and a MAD of 410.70 kg/ha (Fig. 9b). In comparison, the WOFOST-EW model outperformed the WOFOST model, achieving a Pearson's r of 0.91, an $R^2$ of 0.80, an RMSE of 555.72 kg/ha, and a MAD of

https://doi.org/10.5194/egusphere-2024-4010
Preprint. Discussion started: 25 February 2025


333.52 kg/ha (Fig. 9b). The WOFOST-EW model is better equipped to capture the impact of extreme weather on wheat yield. The WOFOST-EW model demonstrates lower uncertainty and delivers more accurate simulation results (Figs. 8 and 9).

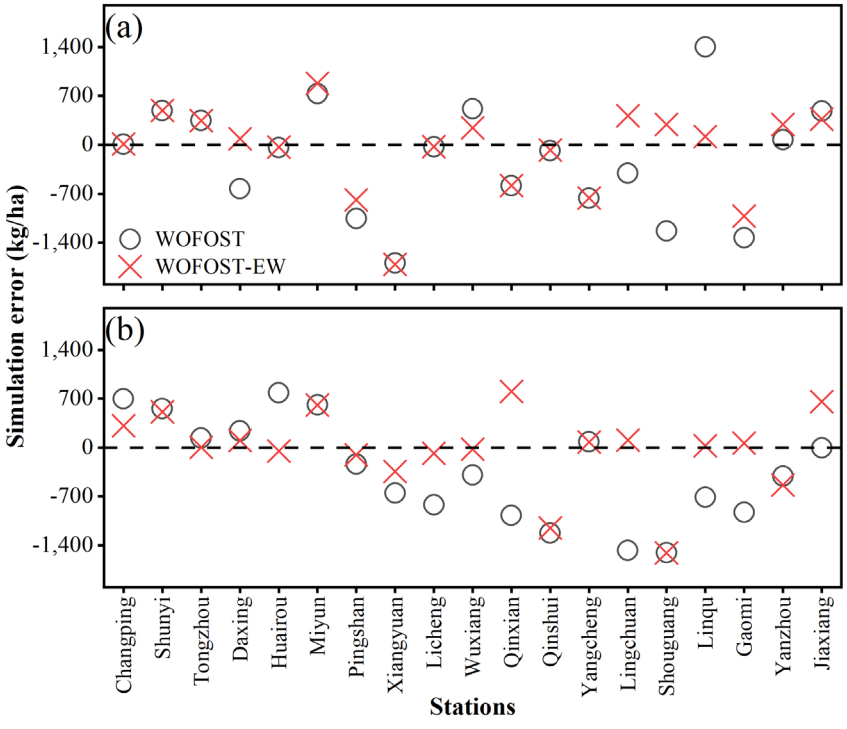


**Figure 9.** Distribution of simulation errors of the WOFOST model and WOFOST-EW in the counties affected by extreme weather in 2008 (a) and 2018 (b).

## 4 Discussion

### 4.1 Impact of extreme weather events on the growth of winter wheat

Extreme weather events such as heatwaves, frosts, droughts, and floods have a significant impact on crop growth and yields (Lüttger and Feike, 2017; Xiao et al., 2018). In this study, we used seven climate indices to quantify extreme climate conditions and observed differences in the impact of extreme weather across different counties (Fig. 5, S1, and S2). During the wheat growing season in the North China Plain, HDD and LDD fluctuated significantly, indicating that wheat often faces severe heat stress and cold stress. This finding is consistent with previous research, which indicated that winter wheat is often affected by extreme low-temperature events before flowering and extreme high-temperature events after flowering, with a negative impact

https://doi.org/10.5194/egusphere-2024-4010
Preprint. Discussion started: 25 February 2025


on wheat yields (Bai et al., 2024). Frost events during the jointing and booting stages also have a significant impact on winter wheat, leading to reduced spike numbers, and resulting in significant yield losses (Li et al., 2015; Ji et al., 2017). During flowering or grain-filling stages, heat stress often leads to grain sterility, reducing the grain count, and persistent heat stress can result in significant yield losses (Lobell et al., 2015; Liu et al., 2016).

Compared to HDD and LDD, R95P, R10mm, and Rx1day showed little fluctuation across various counties in the study area, tending towards stability (Figs. 5 and S1). This is mainly because the precipitation season in the North China Plain does not coincide with the winter wheat growing season (Bai et al., 2024), and extreme precipitation events are unevenly distributed in time and space in the North China Plain (Bai et al., 2022). However, despite this, wheat growth periods are still subject to extreme precipitation stress (Table S1), especially against the backdrop of global warming, future changes in extreme weather events may increase the risks to wheat production.

### 4.2 Uncertainty in simulation results

The uncertainty of crop model parameters is a complex and significant issue, with limited empirical data on crop development rates under extreme temperature conditions being a key factor. Previous studies have shown that the parameters of temperature response functions largely depend on field experimental data; however, these data often lack coverage of extreme temperature environments (Watts, 1971; Tollenaar, 1979; Ellis et al., 1992; Zhang and Tao, 2019). A recent study (Zheng and Zhang, 2025) suggested that the increasing frequency of extreme weather events could cause greater fluctuations in meteorological data, making the input parameters required by models unstable. This instability may lead to deviations in model outputs, ultimately affecting the accuracy of crop growth predictions. Additionally, obtaining reliable crop simulation parameters under extreme weather conditions is highly challenging. For example, extreme weather events such as high and low-temperature fluctuations in the North China Plain can destabilize meteorological data and input parameters, resulting in uncertainty in crop model predictions and making it difficult to accurately simulate crop growth under such conditions.

In response to these challenges, we proposed the WOFOST-EW model to quantify extreme weather events and address the lack of extreme temperature data in traditional crop models. This improved model demonstrated lower uncertainty and reduced fluctuation in simulation results. The phenological simulation results (Fig. 4) and yield simulation results (Figs. 7, 8, and 9) showed that the improved model simulated crop growth more accurately, reducing bias and increasing the model's reliability.

Our research not only enhances the crop model but also provides a solution to the core issue of model parameter uncertainty. By incorporating extreme weather events into the simulation framework, we successfully reduced the model's uncertainty, offering a feasible pathway for more accurate crop growth simulations.

https://doi.org/10.5194/egusphere-2024-4010
Preprint. Discussion started: 25 February 2025


### 4.3 Advantages and limitations of the WOFOST-EW model

In this study, we developed the F(EW) function, leveraging climate indices and LSTM algorithms, and successfully integrated it into the WOFOST model. The results demonstrate that the WOFOST-EW model significantly enhanced yield prediction accuracy in the counties im d by extreme weather events (Figs. 8 and 9). By incorporating climate indices, the model effectively captured wheat growth dynamics under varying environmental conditions, enabling a more accurate representation of climate change impacts on yield. A comprehensive evaluation of s tions from 1990 to 2020 highlighted the exceptional performance of the improved WOFOST model in predicting both long-term trends and annual yields. These findings confirm that the F(EW) function is a robust approach for enhancing model performance. Future research could explore its potential applications across other crops and regions to broaden its utility. Further analysis revealed that the WOFOST-EW del excelled in simulating wheat yields under extreme climate conditions. Notably, extreme weather events in 2008 and 2018 posed significant challenges for traditional modeling approaches. However, the improved model demonstrated a substantial increase in simulation accuracy by integrating climate indices and LSTM algorithms (Figs. 8 and 9).

Previous studies have attempted to estimate the impact of extreme weather events on crop yields using machine learning methods. However, most of these studies relied on outputs from crop models as inputs for machine learning (Feng et al., 2019; Shahhosseini et al., 2021; Li et al., 2023; Zhuang et al., 2024). The unique strength of our model lies in its innovative integration of extreme weather functions, which enhances its ability to more accurately capture the effects of extreme weather events on wheat yields, theoretically improving prediction accuracy. The WOFOST-EW model not only performs well under ge climatic conditions but also exhibits strong adaptability and robustness in addressing extreme climate events. The F(EW) function effectively captures wheat growth dynamics across diverse environmental conditions, providing more precise yield predictions under extreme weather scenarios. In addition, WOFOST-EW has broad applicability, capable of being extended to regions beyond the North China Plain and can be applied to other crops. Future research could further optimize the model by incorporating more environmental and management data, thereby enhancing its adaptability and prediction accuracy under a wider range of conditions.

However, during validation, the WOFOST-EW model underperformed in several counties (Tabl and S4). Further investigation revealed that the primary reason for this was that, due to data limitations, we only accounted for the heading and maturity stages and omitted other key phenological periods of winter wheat. This incomplete consideration of growth stages likely impacted the model's ability to fully capture the crop's growth dynamics under varying conditions. Previous studies have shown that the effects of extreme climate events on crop production vary across different growth stages (Porter and Gawith, 1999; Tack et al., 2015; Feng et al., 2019). During the wheat growth cycle, different stages experience varying types and intensities of climatic stress, resulting in significant differences in yield impacts. Moreover, severe droughts occurring during

https://doi.org/10.5194/egusphere-2024-4010
Preprint. Discussion started: 25 February 2025


the critical growth stages from April to May are particularly likely to affect winter wheat yields (Xu et al., 2018; Yang et al., 2020). Additionally, a series of studies on different crop types and regions have demonstrated that crop yields are more vulnerable to droughts occurring during key growth stages (Potopova et al., 2015; Zipper et al., 2016; Pena-Gallardo et al., 2018). This phenomenon can be attributed to two main factors: (1) physiological differences and variations in field management practices across phenological stages (Wu et al., 2004), which result in distinct drought resistance capacities at different growth stages (Nesmith and Ritchie, 1992); and (2) the varying impacts of droughts on yield formation depending on the growth stage at which they occur (Zhao, 2001). This presents an important direction for future research and model improvement. By further refining the model to account for specific types and intensities of climatic stress at different growth stages, we can enhance prediction accuracy and better capture the impacts of extreme weather events on wheat yields.

Previous studies have highlighted a limitation of the PDSI, which does not consider field management practices in its input parameters, reducing its effectiveness in assessing the impacts of drought on crop growth (Wu et al., 2023). Our study addresses this shortcoming by integrating a crop model, thereby improving the evaluation of drought effects on crop yields. However, this study does not explore in-depth the lag effects of different types of droughts on crop growth, which may affect the identification of sensitive periods in the winter wheat growth cycle. Another limitation of the WOFOST-EW model is its failure to consider the impacts of pests, diseases, and lodging, which could lead to inaccurate yield predictions. Future research will integrate pest and disease data and use high-resolution climate forecast data to optimize the model. Additionally, efforts will focus on reducing irrigation dependence through improved drought prevention and precision management, promoting sustainable agricultural practices. These improvements will enhance the model's practicality and provide reliable support for drought-resistant agricultural production and food security.

## 5 Conclusion

In this study, we introduced the WOFOST-EW model by integrating extreme weather indices with the LSTM deep learning algorithm, aiming to improve the simulation of crop yield and phenology under extreme weather conditions, thereby enhancing its accuracy and robustness. Validation results from 25 stations in the study area over the period 1980-2020 show that the WOFOST-EW model outperformed the OST model in both yield and p logy simulations. Specifically, WOFOST-EW improved prediction accuracy by 10.64 % in the heading stage and 12.86 % in the maturity stage, respectively (Fig. 4). Additionally, the WOFOST-EW model exhibited smaller errors in phenology simulations (Fig. 4c), indicating increased robustness. In yield simulations, WOFOST-EW reduced the RMSE from 665.76 kg/ha to 565.63 kg/ha, and the $R^2$ improved from 0.67 to 0.76 (Fig. 7).

https://doi.org/10.5194/egusphere-2024-4010
Preprint. Discussion started: 25 February 2025


In the extreme weather years of 2008 and 2018, WOFOST-EW demonstrated better simulation capabilities. In 2008, WOFOST-EW reduced the RMSE from 799.99 kg/ha to 617.05 kg/ha and improved the $R^2$ from 0.69 to 0.79 (Fig. 8). Similarly, in 2018, WOFOST-EW decreased the RMSE from 880.33 kg/ha to 555.72 kg/ha and increased the $R^2$ from 0.61 to 0.80 (Fig. 8). The WOFOST-EW model we proposed not only enhances the simulation capability of crop growth under extreme weather events but also improves its robustness and accuracy. As extreme weather events become more frequent in the future, our model holds significant potential for application. WOFOST-EW model can help decision-makers more accurately assess the potential impacts of these events on crop yields, thereby supporting more effective agricultural planning and risk management. This will provide practical experience and technical support for the adaptation of agricultural systems and their sustainable development in the context of global climate change.

*Code availability.* The WOFOST model used in this study is from version 6.0.6 of the PCSE (De Wit, 2018; De Wit et al., 2025), available at https://doi.org/10.5281/zenodo.14785412. The upgraded WOFOST-EW model used in this study can be obtained at https://doi.org/10.5281/zenodo.14859629 (Zheng, 2025). The SCE-UA algorithm (Duan et al., 1992; Duan et al., 1993; Houska et al., 2018) can be referenced at https://doi.org/10.5281/zenodo.7683999. The LSTM model (Hochreiter and Schmidhuber, 1997) is implemented using the "Keras" library (Chollet et al., 2025) provided by Python, available at https://doi.org/10.5281/zenodo.14785196.

*Data availability.* All data used in this paper are available and have been fully referenced in the text.

*Author contributions.* L.Y. designed the project. J.Z. developed the model code with help from L.Y., Z.D., and L.X. J.Z. wrote an initial draft of the paper. L.Y., Z.D., and L.X. supervised the research, co-designed the experiments, and contributed to the manuscript. All authors participated in interpreting the results and refining the paper.

*Competing interests.* At least one of the (co-)authors is a member of the editorial board of *Geoscientific Model Development*.

*Acknowledgments.* The authors would like to thank Wenchao Qi, Tao Liu, and Xiyu Li for their support and contributions to this work.

*Financial support.* This work is supported by the National Key R&D Program of China (grant number: 2022YFE0195900) and the National Key Scientific and Technological Infrastructure project "Earth System Science Numerical Simulator Facility" (EarthLab).

**References**

Ai, Z., Hanasaki, N., Heck, V., Hasegawa, T., and Fujimori, S.: Simulating second-generation herbaceous bioenergy crop yield

https://doi.org/10.5194/egusphere-2024-4010
Preprint. Discussion started: 25 February 2025


using the global hydrological model H08 (v.bio1), Geosci. Model Dev., 13, 6077-6092, https://doi.org/10.5194/gmd-13-6077-2020, 2020.

Ai, Z., and Hanasaki, N.: Simulation of crop yield using the global hydrological model H08 (crp.v1), Geosci. Model Dev., 16, 3275-3290, https://doi.org/10.5194/gmd-16-3275-2023, 2023.

Ali, T., Huang, J., Wang, J., and Xie, W.: Global footprints of water and land resources through China's food trade, Global food security, 12, 139-145, https://doi.org/https://doi.org/10.1016/j.gfs.2016.11.003, 2017.

Al-Sakkaf, A. S., Zhang, J., Yao, F., Hamed, M. M., Simbi, C. H., Ahmed, A., and Shahid, S.: Assessing Exposure to Climate Extremes over the Arabian Peninsula Using Era5 Reanalysis Data: Spatial Distribution and Temporal Trends, Atmos. Res., 300, 107224, https://doi.org/10.1016/j.atmosres.2024.107224, 2024.

Bai, H., Jianzhao, T., Wang, B., Cao, J., and Feng, P.: Projecting Future Changes in Extreme Climate for Maize Production in the North China Plain and the Role of Adjusting the Sowing Date, Mitig. Adapt. Strateg. Glob. Chang., 27, 21, https://doi.org/10.1007/s11027-022-09995-4, 2022.

Bai, H., Xiao, D., Tang, J., and De Li Liu: Evaluation of Wheat Yield in North China Plain under Extreme Climate by Coupling Crop Model with Machine Learning, Comput. Electron. Agric., 217, 108651, https://doi.org/10.1016/j.compag.2024.108651, 2024.

Bai, H., Xiao, D., Wang, B., De Li Liu, and Tang, J.: Simulation of Wheat Response to Future Climate Change Based on Coupled Model Inter-Comparison Project Phase 6 Multi-Model Ensemble Projections in the North China Plain, Front. Plant Sci., 13, 829580, https://doi.org/10.3389/fpls.2022.829580, 2022.

Beyene, A. N., Zeng, H., Wu, B., Zhu, L., Gebremicael, T. G., Zhang, M., and Bezabh, T.: Coupling remote sensing and crop growth model to estimate national wheat yield in Ethiopia, Big Earth Data, 6, 18-35, https://doi.org/10.1080/20964471.2020.1837529, 2022.

Boori, M. S., Choudhary, K., Paringer, R., and Kupriyanov, A.: Machine Learning for Yield Prediction in Fergana Valley, Central Asia, Journal of the Saudi Society of Agricultural Sciences, 22, 107-120, https://doi.org/10.1016/j.jssas.2022.07.006, 2022.

Cao, J., Zhang, Z., Tao, F., Zhang, L., Luo, Y., Zhang, J., Han, J., and Xie, J.: Integrating Multi-Source Data for Rice Yield Prediction Across China Using Machine Learning and Deep Learning Approaches, Agric. For. Meteorol., 297, 108275, https://doi.org/10.1016/j.agrformet.2020.108275, 2021.

Chen, Y., Zhang, Z., and Tao, F.: Improving Regional Winter Wheat Yield Estimation Through Assimilation of Phenology and Leaf Area Index from Remote Sensing Data, Eur. J. Agron., 101, 163-173, https://doi.org/10.1016/j.eja.2018.09.006, 2018.

Chenu, K., Porter, J. R., Martre, P., Basso, B., Chapman, S. C., Ewert, F., Bindi, M., and Asseng, S.: Contribution of Crop Models to Adaptation in Wheat, Trends Plant Sci., 22, 472-490, https://doi.org/10.1016/j.tplants.2017.02.003, 2017.

Chollet, F., Gardener, T., Zhu, Q. S., Jin, H., Rahman, F., and Watson, M.: zheng-jinhui/keras (3.8.0), Zenodo [code], https://doi.org/10.5281/zenodo.14785196, 2025.

De Wit, A.: PCSE: the Python crop simulation environment, URL: https://pcse. readthedocs. io/en/stable/(accessed 5 February 2019), 2018.

De Wit, A., Berghuijs, H., Steven, Orzan, I., Fanquake, and Gomez, A.: zheng-jinhui/pcse (6.0.6), Zenodo [code], https://doi.org/10.5281/zenodo.14785412, 2025.

De Wit, A., Boogaard, H. L., Supit, I., and van den Berg, M.: System description of the WOFOST 7.2, cropping systems model, Wageningen Environmental Research, 2020.

de Wit, A., Boogaard, H., Fumagalli, D., Janssen, S., Knapen, R., van Kraalingen, D., Supit, I., van der Wijngaart, R., and van Diepen, K.: 25 Years of the WOFOST Cropping Systems Model, Agric. Syst., 168, 154-167, https://doi.org/10.1016/j.agsy.2018.06.018, 2018.

De Wit, A., and Boogaard, H.: A gentle introduction to WOFOST, Wageningen Environmental Research, November, https://www. wur. nl/en/research-results/research-institutes/environmental-research/facilities-tools/software-models-and-databases/wofost/documentation-wofost. htm (last access: October 2022), 2021.

Dinh, T. L. A., and Aires, F.: Nested Leave-Two-out Cross-Validation for the Optimal Crop Yield Model Selection, Geosci.

https://doi.org/10.5194/egusphere-2024-4010
Preprint. Discussion started: 25 February 2025


Model Dev., 15, 3519-3535, https://doi.org/10.5194/gmd-15-3519-2022, 2022.
Dong, X., Zhang, T., Yang, X., Li, T., and Li, X.: Rice Yield Benefits from Historical Climate Warming to Be Negated by Extreme Heat in Northeast China, Int. J. Biometeorol., 67, 835-846, https://doi.org/10.1007/s00484-023-02458-8, 2023.
Duan, Q. Y., Gupta, V. K., and Sorooshian, S.: Shuffled complex evolution approach for effective and efficient global minimization, J. Optim. Theory Appl., 76, 501-521, https://doi.org/https://doi.org/10.1007/BF00939380, 1993.
Duan, Q., Sorooshian, S., and Gupta, V. K.: Optimal use of the SCE-UA global optimization method for calibrating watershed models, J. Hydrol., 158, 265-284, https://doi.org/https://doi.org/10.1016/0022-1694(94)90057-4, 1994.
Duan, Q., Sorooshian, S., and Gupta, V.: Effective and efficient global optimization for conceptual rainfall-runoff models, Water Resour. Res., 28, 1015-1031, https://doi.org/ https://doi.org/10.1029/91WR02985, 1992.
Ellis, R. H., Summerfield, R. J., Edmeades, G. O., and Roberts, E. H.: Photoperiod, Temperature, and the Interval from Sowing to Tassel Initiation in Diverse Cultivars of Maize, Crop Sci., 32, 1225-1232, https://doi.org/https://doi.org/10.2135/cropsci1992.0011183X003200050033x, 1992.
Erenstein, O., Jaleta, M., Mottaleb, K. A., Sonder, K., Donovan, J., and Braun, H.: Global trends in wheat production, consumption and trade, in: Wheat improvement: food security in a changing climate, edited, Springer International Publishing Cham, 47-66, 2022.
Fao: Food and Agriculture Organization of the United Nations, Roma: FAO, 2021.
Farooq, M., Bramley, H., Palta, J. A., and Siddique, K. H. M.: Heat Stress in Wheat During Reproductive and Grain-Filling Phases, Crit. Rev. Plant Sci., 30, 491-507, https://doi.org/10.1080/07352689.2011.615687, 2011.
Feng, P., Wang, B., De Li Liu, Waters, C., and Yu, Q.: Incorporating machine learning with biophysical model can improve the evaluation of climate extremes impacts on wheat yield in south-eastern Australia, Agric. For. Meteorol., 275, 100-113, https://doi.org/10.1016/j.agrformet.2019.05.018, 2019.
Feng, P., Wang, B., Li Liu, D., Waters, C., and Yu, Q.: Incorporating machine learning with biophysical model can improve the evaluation of climate extremes impacts on wheat yield in south-eastern Australia, Agric. For. Meteorol., 275, 100-113, 2019.
Fu, J., Jian, Y., Wang, X., Li, L., Ciais, P., Zscheischler, J., Wang, Y., Tang, Y., Müller, C., Webber, H., Yang, B., Wu, Y., Wang, Q., Cui, X., Huang, W., Liu, Y., Zhao, P., Piao, S., and Zhou, F.: Extreme rainfall reduces one-twelfth of China's rice yield over the last two decades, Nat. Food, 4, 416-426, https://doi.org/10.1038/s43016-023-00753-6, 2023.
Guo, H., Hu, W., Yang, C., and Wan, F.: Moisture Sources and Atmospheric Circulation Patterns for Extreme Rainfall Event over North China Plain from 29 July to 2 August 2023, Earth Space Sci., 11, e2024EA003956, https://doi.org/10.1029/2024ea003956, 2024.
Han, J., Zhang, Z., Cao, J., Luo, Y., Zhang, L., Li, Z., and Zhang, J.: Prediction of Winter Wheat Yield Based on Multi-Source Data and Machine Learning in China, Remote Sens., 12, 236, https://doi.org/10.3390/rs12020236, 2020.
Heinicke, S., Frieler, K. A., Jagermeyr, J., and Mengel, M.: Global gridded crop models underestimate yield responses to droughts and heatwaves, Environ. Res. Lett., 17, 44026, https://doi.org/10.1088/1748-9326/ac592e, 2022.
Hochreiter, S., and Schmidhuber, J.: Long Short-term Memory, Neural Computation MIT-Press, 1997.
Hong, Y., and Ying, S.: Characteristics of Extreme Temperature and Precipitation in China in 2017 Based on ETCCDI Indices, Adv. Clim. Chang. Res., 9, 218-226, https://doi.org/10.1016/j.accre.2019.01.001, 2018.
Houska, T., Kraft, P., Chamorro-Chavez, A., and Breuer, L.: SPOTPY: A python tool for sensitivity and uncertainty analysis of environmental models, 2018-1-1, 7470, 2018.
Hu, S., Mo, X., and Lin, Z.: The Contribution of Climate Change to the Crop Phenology and Yield in Haihe River Basin, Geogr. Res., 33, 3-12, 2014.
Huang, L., Wang, L., Zhang, Y., Xing, L., Hao, Q., Xiao, Y., Yang, L., and Zhu, H.: Identification of Groundwater Pollution Sources by a SCE-UA Algorithm-Based Simulation/Optimization Model, Water, 10, 193, https://doi.org/10.3390/w10020193, 2018.
Iniyan, S., Akhil Varma, V., and Teja Naidu, C.: Crop yield prediction using machine learning techniques, Adv. Eng. Softw., 175, 103326, https://doi.org/10.1016/j.advengsoft.2022.103326, 2023.
Ji, H., Xiao, L., Xia, Y., Song, H., Liu, B., Tang, L., Cao, W., Zhu, Y., and Liu, L.: Effects of jointing and booting low

temperature stresses on grain yield and yield components in wheat, Agric. For. Meteorol., 243, 33-42, https://doi.org/10.1016/j.agrformet.2017.04.016, 2017.

Ji, Z., Pan, Y., Zhu, X., Zhang, D., and Wang, J.: A Generalized Model to Predict Large-Scale Crop Yields Integrating Satellite-Based Vegetation Index Time Series and Phenology Metrics, Ecol. Indic., 137, 108759, https://doi.org/10.1016/j.ecolind.2022.108759, 2022.

Kalchbrenner, N. E., Danihelka, I., and Graves, A. B.: Grid long short-term memory neural networks, Neural Comput., 9, 1735-1780, https://doi.org/10.1162/neco.1997.9.8.1735, 2019.

Khanal, S., Fulton, J., Klopfenstein, A., Douridas, N., and Shearer, S.: Integration of High Resolution Remotely Sensed Data and Machine Learning Techniques for Spatial Prediction of Soil Properties and Corn Yield, Comput. Electron. Agric., 153, 213-225, https://doi.org/10.1016/j.compag.2018.07.016, 2018.

Lesk, C., Rowhani, P., and Ramankutty, N.: Influence of Extreme Weather Disasters on Global Crop Production, Nature, 529, 84-87, https://doi.org/10.1038/nature16467, 2016.

Li, L., Zhang, Y., Wang, B., Feng, P., He, Q., Shi, Y., Liu, K., Harrison, M. T., De Li Liu, Yao, N., Li, Y., He, J., Feng, H., Siddique, K. H. M., and Yu, Q.: Integrating Machine Learning and Environmental Variables to Constrain Uncertainty in Crop Yield Change Projections under Climate Change, Eur. J. Agron., 149, 126917, https://doi.org/10.1016/j.eja.2023.126917, 2023.

Li, N., Lin, H., Wang, T., Li, Y., Liu, Y., Chen, X., and Hu, X.: Impact of climate change on cotton growth and yields in Xinjiang, China, Field Crops Res., 247, 107590, https://doi.org/https://doi.org/10.1016/j.fcr.2019.107590, 2020.

Li, X., Cai, J., Liu, F., Dai, T., Cao, W., and Jiang, D.: Spring Freeze Effect on Wheat Yield is Modulated by Winter Temperature Fluctuations: Evidence from Meta-Analysis and Simulating Experiment, J. Agron. Crop Sci., 201, 288-300, https://doi.org/10.1111/jac.12115, 2014.

Li, X., Pu, H., Liu, F., Zhou, Q., Cai, J., Dai, T., Cao, W., and Jiang, D.: Winter Wheat Photosynthesis and Grain Yield Responses to Spring Freeze, Agron. J., 107, 1002-1010, https://doi.org/10.2134/agronj14.0460, 2015.

Li, X., Tan, J., Wang, X., Han, G., Qian, Z., Li, H., Wang, L., and Niu, G.: Responses of Spring Wheat Yield and Growth Period to Different Future Climate Change Models in the Yellow River Irrigation Area Based on CMIP6 and WOFOST Models, Agric. For. Meteorol., 353, 110071, https://doi.org/10.1016/j.agrformet.2024.110071, 2024.

Li, Z., Qing-Quan, C., Yu-Lin, J., Fu, C., and Yong-Deng, L.: Impacts of Climate Change on Drought Risk of Winter Wheat in the North China Plain, J. Integr. Agric., 20, 2601-2612, https://doi.org/10.1016/s2095-3119(20)63273-7, 2021.

Liu, B., Asseng, S., Liu, L., Tang, L., Cao, W., and Zhu, Y.: Testing the Responses of Four Wheat Crop Models to Heat Stress at Anthesis and Grain Filling., Glob. Change Biol., 22, 1890-1903, https://doi.org/10.1111/gcb.13212, 2016.

Liu, B., Liu, L., Tian, L., Cao, W., Zhu, Y., and Asseng, S.: Post-heading Heat Stress and Yield Impact in Winter Wheat of China., Glob. Change Biol., 20, 372-381, https://doi.org/10.1111/gcb.12442, 2013.

Liu, K., Harrison, M. T., Shabala, S., Meinke, H., Ahmed, I., Zhang, Y., Tian, X., and Zhou, M.: The State of the Art in Modeling Waterlogging Impacts on Plants: What Do We Know and What Do We Need to Know, Earth Future, 8, n/a-n/a, https://doi.org/10.1029/2020ef001801, 2020.

Lobell, D. B., Hammer, G. L., Chenu, K., Zheng, B., Mclean, G., and Chapman, S. C.: The Shifting Influence of Drought and Heat Stress for Crops in Northeast Australia, Glob. Change Biol., 21, 4115-4127, https://doi.org/10.1111/gcb.13022, 2015.

Lobell, D. B., Schlenker, W., and Costa-Roberts, J.: Climate trends and global crop production since 1980, Science, 333, 616-620, 2011.

Lobell, D. B., and Burke, M. B.: On the Use of Statistical Models to Predict Crop Yield Responses to Climate Change, Agric. For. Meteorol., 150, 1443-1452, https://doi.org/10.1016/j.agrformet.2010.07.008, 2010.

Lu, Y., and Yang, X.: Using the anomaly forcing Community Land Model (CLM 4.5) for crop yield projections, Geosci. Model Dev., 14, 1253-1265, https://doi.org/10.5194/gmd-14-1253-2021, 2021.

Lüttger, A. B., and Feike, T.: Development of Heat and Drought Related Extreme Weather Events and Their Effect on Winter Wheat Yields in Germany, Theor. Appl. Climatol., 132, 15-29, https://doi.org/10.1007/s00704-017-2076-y, 2017.

Ma, Y., Zhang, Z., Kang, Y., and Ozdogan, M.: Corn yield prediction and uncertainty analysis based on remotely sensed variables using a Bayesian neural network approach, Remote Sens. Environ., 259, 112408,

https://doi.org/10.5194/egusphere-2024-4010
Preprint. Discussion started: 25 February 2025


https://doi.org/10.1016/j.rse.2021.112408, 2021.
Maimaitijiang, M., Sagan, V., Sidike, P., Hartling, S., Esposito, F., and Fritschi, F. B.: Soybean Yield Prediction from UAV Using Multimodal Data Fusion and Deep Learning, Remote Sens. Environ., 237, 111599, https://doi.org/10.1016/j.rse.2019.111599, 2019.
Mo, X., Hu, S., Lin, Z., Liu, S., and Xia, J.: Impacts of Climate Change on Agricultural Water Resources and Adaptation on the North China Plain, Adv. Clim. Chang. Res., 8, 93-98, https://doi.org/10.1016/j.accre.2017.05.007, 2017.
Nesmith, D. S., and Ritchie, J. T.: Maize (zea Mays L.) Response to a Severe Soil Water-Deficit During Grain-Filling, Field Crops Res., 29, 23-35, https://doi.org/10.1016/0378-4290(92)90073-i, 1992.
Osman, R., Zhu, Y., Ma, W., Zhang, D., Ding, Z., Liu, L., Tang, L., Liu, B., and Cao, W.: Comparison of Wheat Simulation Models for Impacts of Extreme Temperature Stress on Grain Quality, Agric. For. Meteorol., 288-289, 107995, https://doi.org/10.1016/j.agrformet.2020.107995, 2020.
Panigrahy, S.: SMOTE-based Deep LSTM System with GridSearchCV Optimization for Intelligent Diabetes Diagnosis, J. Electr. Syst., 20, 804-815, https://doi.org/10.52783/jes.3455, 2024.
Pei, J., Tan, S., Zou, Y., Liao, C., He, Y., Wang, J., Huang, H., Wang, T., Tian, H., Fang, H., Wang, L., and Huang, J.: The Role of Phenology in Crop Yield Prediction: Comparison of Ground-Based Phenology and Remotely Sensed Phenology, Agric. For. Meteorol., 361, 110340, https://doi.org/10.1016/j.agrformet.2024.110340, 2025.
Pena-Gallardo, M., Vicente-Serrano, S. M., Quiring, S., Svoboda, M., Hannaford, J., Tomas-Burguera, M., Martin-Hernandez, N., Dominguez-Castro, F., and Kenawy, A. E.: Response of Crop Yield to Different Time-Scales of Drought in the United States: Spatio-temporal Patterns and Climatic and Environmental Drivers, Agric. For. Meteorol., 264, 40-55, https://doi.org/10.1016/j.agrformet.2018.09.019, 2018.
Porter, J. R., and Gawith, M.: Temperatures and the Growth and Development of Wheat: A Review, Eur. J. Agron., 10, 23-36, https://doi.org/10.1016/s1161-0301(98)00047-1, 1999.
Potopova, V., Stepanek, P., Mozny, M., Tuerkott, L., and Soukup, J.: Performance of the Standardised Precipitation Evapotranspiration Index at Various Lags for Agricultural Drought Risk Assessment in the Czech Republic, Agric. For. Meteorol., 202, 26-38, https://doi.org/10.1016/j.agrformet.2014.11.022, 2015.
Powell, J. P., and Reinhard, S.: Measuring the effects of extreme weather events on yields, Weather Clim. Extremes, 12, 69-79, https://doi.org/10.1016/j.wace.2016.02.003, 2016.
Ray, D. K., Gerber, J. S., Macdonald, G. K., and West, P. C.: Climate Variation Explains a Third of Global Crop Yield Variability., Nat. Commun., 6, 5989, https://doi.org/10.1038/ncomms6989, 2015.
Reynolds, M. P., Slafer, G. A., Foulkes, J. M., Griffiths, S., Murchie, E. H., Carmo-Silva, E., Asseng, S., Chapman, S. C., Sawkins, M., Gwyn, J., and Flavell, R. B.: Author Correction: A Wiring Diagram to Integrate Physiological Traits of Wheat Yield Potential, Nat. Food, 3, 665, https://doi.org/10.1038/s43016-022-00574-z, 2022.
Rezaei, E. E., Siebert, S., Manderscheid, R., Mueller, J., Mahrookashani, A., Ehrenpfordt, B., Haensch, J., Weigel, H., and Ewert, F.: Quantifying the Response of Wheat Yields to Heat Stress: the Role of the Experimental Setup, Field Crops Res., 217, 93-103, https://doi.org/10.1016/j.fcr.2017.12.015, 2018.
Ringeval, B., Mueller, C., Pugh, T. A. M., Mueller, N. D., Ciais, P., Folberth, C., Liu, W., Debaeke, P., and Pellerin, S.: Potential Yield Simulated by Global Gridded Crop Models: Using a Process-Based Emulator to Explain Their Differences, Geosci. Model Dev., 14, 1639-1656, https://doi.org/10.5194/gmd-14-1639-2021, 2021.
Roberts, M. J., Braun, N. O., Sinclair, T. R., Lobell, D. B., and Schlenker, W.: Comparing and Combining Process-Based Crop Models and Statistical Models with Some Implications for Climate Change, Environ. Res. Lett., 12, 95010, https://doi.org/10.1088/1748-9326/aa7f33, 2017.
Ruan, G., Li, X., Yuan, F., Cammarano, D., Ata-Ui-Karim, S. T., Liu, X., Tian, Y., Zhu, Y., Cao, W., and Cao, Q.: Improving wheat yield prediction integrating proximal sensing and weather data with machine learning, Comput. Electron. Agric., 195, 106852, https://doi.org/10.1016/j.compag.2022.106852, 2022.
Shahhosseini, M., Hu, G., Huber, I., and Archontoulis, S. V.: Coupling Machine Learning and Crop Modeling Improves Crop Yield Prediction in the US Corn Belt, Sci. Rep., 11, 1606, https://doi.org/10.1038/s41598-020-80820-1, 2021.
Shen, R., Dong, J., Yuan, W., Han, W., Ye, T., and Zhao, W.: A 30 m Resolution Distribution Map of Maize for China Based

https://doi.org/10.5194/egusphere-2024-4010
Preprint. Discussion started: 25 February 2025


on Landsat and Sentinel Images, Journal of Remote Sensing, 2022, https://doi.org/10.34133/2022/9846712, 2022.
Shi, J., Wang, Z., Zhang, Z., Fei, Y., Li, Y., Zhang, F. E., Chen, J., and Qian, Y.: Assessment of Deep Groundwater Over-Exploitation in the North China Plain, Earth Sci. Front., 2, 593-598, https://doi.org/10.1016/j.gsf.2011.07.002, 2011.
Singh Boori, M., Choudhary, K., Paringer, R., and Kupriyanov, A.: Machine learning for yield prediction in Fergana valley, Central Asia, Journal of the Saudi Society of Agricultural Sciences, 22, 107-120, https://doi.org/10.1016/j.jssas.2022.07.006, 2023.
Song, Y., Linderholm, H. W., Wang, C., Tian, J., Huo, Z., Gao, P., Song, Y., and Guo, A.: The Influence of Excess Precipitation on Winter Wheat under Climate Change in China from 1961 to 2017., The Science of The Total Environment, 690, 189-196, https://doi.org/10.1016/j.scitotenv.2019.06.367, 2019.
Sun, J., Lai, Z., Di, L., Sun, Z., Tao, J., and Shen, Y.: Multilevel deep learning network for county-level corn yield estimation in the us corn belt, IEEE J. Sel. Top. Appl. Earth Observ. Remote Sens., 13, 5048-5060, https://doi.org/10.1109/JSTARS.2020.3019046, 2020.
Supit, I., Hooijer, A. A., and Van Diepen, C. A.: System description of the WOFOST 6.0 crop simulation model implemented in CGMS, vol. 1: Theory and Algorithms, Joint Research Centre, Commission of the European Communities, EUR, 15956, 146, 1994.
Tack, J., Barkley, A., and Nalley, L. L.: Effect of Warming Temperatures on US Wheat Yields, Proc. Natl. Acad. Sci. U. S. A., 112, 6931-6936, https://doi.org/10.1073/pnas.1415181112, 2015.
Tang, R., Supit, I., Hutjes, R., Zhang, F., Wang, X., Chen, X., Zhang, F., and Chen, X.: Modelling Growth of Chili Pepper (capsicum Annuum L.) with the WOFOST Model, Agric. Syst., 209, 103688, https://doi.org/10.1016/j.agsy.2023.103688, 2023.
Tao, F., Zhang, Z., Zhang, S., Zhu, Z., and Shi, W.: Response of crop yields to climate trends since 1980 in China, Clim. Res., 54, 233-247, https://doi.org/https://doi.org/10.3354/cr01131, 2012.
Tian, H., Wang, P., Tansey, K., Zhang, J., Zhang, S., and Li, H.: An LSTM neural network for improving wheat yield estimates by integrating remote sensing data and meteorological data in the Guanzhong Plain, PR China, Agric. For. Meteorol., 310, 108629, https://doi.org/10.1016/j.agrformet.2021.108629, 2021.
Tollenaar, M.: Effect of Temperature on Rate of Leaf Appearance and Flowering Date in Maize, Crop Sci., 19, 1979.
Torsoni, G. B., de Oliveira Aparecido, L. E., Santos, G. M. D., Chiquitto, A. G., Moraes, J. R. D. S., and de Souza Rolim, G.: Correction To: Soybean Yield Prediction by Machine Learning and Climate, Theor. Appl. Climatol., 151, 1709-1725, https://doi.org/10.1007/s00704-023-04389-1, 2023.
Wang, B., Waters, C., Orgill, S., Cowie, A., Clark, A., De Li Liu, Simpson, M., Mcgowen, I., and Sides, T.: Estimating Soil Organic Carbon Stocks Using Different Modelling Techniques in the Semi-Arid Rangelands of Eastern Australia, Ecol. Indic., 88, 425-438, https://doi.org/10.1016/j.ecolind.2018.01.049, 2018.
Wang, J., Yang, Y., Huang, J., and Adhikari, B.: Adaptive Irrigation Measures in Response to Extreme Weather Events: Empirical Evidence from the North China Plain, Reg. Environ. Change, 19, 1009-1022, https://doi.org/10.1007/s10113-018-1442-3, 2019.
Wang, P., Yang, Li, H., Chen, L., Dang, R., Xue, D., Li, B., Tang, J., Leung, L. R., and Liao, H.: North China Plain As a Hot Spot of Ozone Pollution Exacerbated by Extreme High Temperatures, Atmos. Chem. Phys., 22, 4705-4719, https://doi.org/10.5194/acp-22-4705-2022, 2021.
Wang, T., Li, N., Li, Y., Lin, H., Yao, N., Chen, X., De Li Liu, Yu, Q., and Feng, H.: Impact of Climate Variability on Grain Yields of Spring and Summer Maize, Comput. Electron. Agric., 199, 107101, https://doi.org/10.1016/j.compag.2022.107101, 2022.
Wang, X., Wang, S., Li, X., Chen, B., Wang, J., Huang, M., and Rahman, A.: Modelling Rice Yield with Temperature Optima of Rice Productivity Derived from Satellite NIRv in Tropical Monsoon Area, Agric. For. Meteorol., 294, 108135, https://doi.org/10.1016/j.agrformet.2020.108135, 2020.
Watts, W. R.: Role of Temperature in the Regulation of Leaf Extension in Zea mays, Nature, 229, 46-47, 1971.
Wei, Z., Bian, D., Du, X., Gao, Z., Li, C., Liu, G., Yang, Q., Jiang, A., and Cui, Y.: An Increase in Solar Radiation in the Late Growth Period of Maize Alleviates the Adverse Effects of Climate Warming on the Growth and Development of Maize,

https://doi.org/10.5194/egusphere-2024-4010
Preprint. Discussion started: 25 February 2025


Agronomy, 13, 1284, https://doi.org/10.3390/agronomy13051284, 2023.
Wu, H., Hubbard, K. G., and Wilhite, D. A.: An Agricultural Drought Risk-assessment Model for Corn and Soybeans, Int. J. Climatol., 24, 723-741, https://doi.org/10.1002/joc.1028, 2004.
Wu, J., Wang, N., Xing, X., and Ma, X.: Loss of Net Primary Production of Seasonal Winter Wheat Due to Multiple Drought Types in the Main Grain-Producing Area of China, J. Hydrol., 625, 130093, https://doi.org/10.1016/j.jhydrol.2023.130093, 2023.
Xiao, D., De Li Liu, Wang, B., Feng, P., Bai, H., and Tang, J.: Climate Change Impact on Yields and Water Use of Wheat and Maize in the North China Plain under Future Climate Change Scenarios, Agric. Water Manag., 238, 106238, https://doi.org/10.1016/j.agwat.2020.106238, 2020.
Xiao, L., Liu, L., Asseng, S., Xia, Y., Tang, L., Liu, B., Cao, W., and Zhu, Y.: Estimating Spring Frost and Its Impact on Yield Across Winter Wheat in China, Agric. For. Meteorol., 260, 154-164, https://doi.org/10.1016/j.agrformet.2018.06.006, 2018.
Xiao, L., Wang, G., Wang, E., Liu, S., Chang, J., Zhang, P., Zhou, H., Wei, Y., Zhang, H., Zhu, Y., Shi, Z., and Luo, Z.: Spatiotemporal Co-Optimization of Agricultural Management Practices Towards Climate-Smart Crop Production, Nat. Food, 5, 59-71, https://doi.org/10.1038/s43016-023-00891-x, 2024.
Xu, X., Gao, P., Zhu, X., Guo, W., Ding, J., and Li, C.: Estimating The Responses Of Winter Wheat Yields To Moisture Variations In The Past 35 Years In Jiangsu Province Of China, PLoS One, 13, e0191217, https://doi.org/10.1371/journal.pone.0191217, 2018.
Yang, J., Wu, J., Liu, L., Zhou, H., Gong, A., Han, X., and Zhao, W.: Responses of Winter Wheat Yield to Drought in the North China Plain: Spatial–Temporal Patterns and Climatic Drivers, Water, 12, 3094, https://doi.org/10.3390/w12113094, 2020.
Yang, R., Dai, P., Wang, B., Jin, T., Liu, K., Fahad, S., Harrison, M. T., Man, J., Shang, J., Meinke, H., Liu, D., Wang, X., Zhang, Y., Zhou, M., Tian, Y., and Yan, H.: Over-Optimistic Projected Future Wheat Yield Potential in the North China Plain: the Role of Future Climate Extremes, Agronomy, 12, 145, https://doi.org/10.3390/agronomy12010145, 2022.
Yin, Z., Wang, H., and Che, H.: Understanding Severe Winter Haze Events in the North China Plain in 2014: Roles of Climate Anomalies, Atmos. Chem. Phys., 17, 1641-1651, https://doi.org/10.5194/acp-17-1641-2017, 2017.
Yu, L., Du, Z., Li, X., Zheng, J., Zhao, Q., Wu, H., Weise, D., Yang, Y., Zhang, Q., Li, X., Ma, X., and Huang, X.: Enhancing global agricultural monitoring system for climate-smart agriculture, Climate Smart Agriculture, 2, 100037, https://doi.org/https://doi.org/10.1016/j.csag.2024.100037, 2025.
Zhang, Q., and Miao, C.: A New High-Resolution Multi-Drought Indices Dataset for Mainland China; CHM_Drought, in, edited, figshare, 10.6084/m9.figshare.25656951.v2, 2024.
Zhang, S., Tao, F., and Zhang, Z.: Changes in extreme temperatures and their impacts on rice yields in southern China from 1981 to 2009, Field Crops Res., 189, 43, https://doi.org/10.1016/j.fcr.2016.02.008, 2016.
Zhang, S., Tao, F., and Zhang, Z.: Spatial and temporal changes in vapor pressure deficit and their impacts on crop yields in China during 1980–2008, J. Meteorol. Res., 31, 800-808, 2017a.
Zhang, S., Tao, F., and Zhang, Z.: Uncertainty from model structure is larger than that from model parameters in simulating rice phenology in China, Eur. J. Agron., 87, 30-39, https://doi.org/10.1016/j.eja.2017.04.004, 2017b.
Zhang, S., and Tao, F.: Improving Rice Development and Phenology Prediction Across Contrasting Climate Zones of China, Agric. For. Meteorol., 268, 224-233, https://doi.org/10.1016/j.agrformet.2019.01.019, 2019.
Zhao, S.: Effects of Water Deficits on Yield and WUE in Winter Wheat, Irrig. Drain., 20, 56-69, 2001.
Zhao, Y., Xiao, D., Bai, H., Tang, J., De Li Liu, Qi, Y., and Shen, Y.: The Prediction of Wheat Yield in the North China Plain by Coupling Crop Model with Machine Learning Algorithms, Agriculture, 13, 99, https://doi.org/10.3390/agriculture13010099, 2022.
Zhao, Y., Xu, X., Li, J., Zhang, R., Kang, Y., Huang, W., Xia, Y., Di Liu, and Sun, X.: The Large-Scale Circulation Patterns Responsible for Extreme Precipitation over the North China Plain in Midsummer, Journal of Geophysical Research Atmospheres, 124, 12794-12809, https://doi.org/10.1029/2019jd030583, 2019.
Zheng, J.: zheng-jinhui/WOFOST-EW: Enhanced WOFOST Simulation Model for Extreme Weather (1.0.0), Zenodo [code], https://doi.org/10.5281/zenodo.14782296, 2025.

https://doi.org/10.5194/egusphere-2024-4010
Preprint. Discussion started: 25 February 2025


Zheng, J., and Zhang, S.: Improving Rice Phenology Simulations Based on the Bayesian Model Averaging Method, Eur. J. Agron., 142, 126646, https://doi.org/10.1016/j.eja.2022.126646, 2023.

Zheng, J., and Zhang, S.: Decomposing the total uncertainty in wheat modeling: an analysis of model structure, parameters, weather data inputs, and squared bias contributions, Agric. Syst., 224, 104215, https://doi.org/10.1016/j.agsy.2024.104215, 2025.

Zhuang, H., Zhang, Z., Cheng, F., Han, J., Luo, Y., Zhang, L., Cao, J., Zhang, J., He, B., Xu, J., and Tao, F.: Integrating Data Assimilation, Crop Model, and Machine Learning for Winter Wheat Yield Forecasting in the North China Plain, Agric. For. Meteorol., 347, 109909, https://doi.org/10.1016/j.agrformet.2024.109909, 2024.

Zipper, S. C., Qiu, J., and Kucharik, C. J.: Drought Effects on US Maize and Soybean Production: Spatiotemporal Patterns and Historical Changes, Environ. Res. Lett., 11, 94021, https://doi.org/10.1088/1748-9326/11/9/094021, 2016.